arXiv:1410.7692v1 [stat.ME] 28 Oct 2014

Scalable multiscale density estimation

Ye Wang
Duke University
eric.ye.wang@duke.edu

Antonio Canale
Università degli studi di
Torino e Collegio Carlo Alberto
antonio.canale@unito.it

David Dunson
Duke University
dunson@stat.duke.edu

Abstract

Although Bayesian density estimation using discrete mixtures has good performance in modest dimensions, there is a lack of statistical and computational scalability to high-dimensional multivariate cases. To combat the curse of dimensionality, it is necessary to assume the data are concentrated near a lower-dimensional subspace. However, Bayesian methods for learning this subspace along with the density of the data scale poorly computationally. To solve this problem, we propose an empirical Bayes approach, which estimates a multiscale dictionary using geometric multiresolution analysis in a first stage. We use this dictionary within a multiscale mixture model, which allows uncertainty in component allocation, mixture weights and scaling factors over a binary tree. A computational algorithm is proposed, which scales efficiently to massive dimensional problems. We provide some theoretical support for this geometric density estimation (GEODE) method, and illustrate the performance through simulated and real data examples.

1 Introduction

Let $\boldsymbol{y}_i = (y_{i1}, \ldots, y_{iD})^T$, for $i = 1, \ldots, n$, be a sample from an unknown distribution having support in a subset of $\Re^D$. We are interested in estimating its density when D is large, and the data have a low-dimensional structure with intrinsic dimension p such that $p \ll D$. Kernel methods work well in low dimensions, but face challenges in scaling up to large D settings. In particular, optimally one would allow separate bandwidth parameters for the different variables to accommodate differing smoothness, but then there is the issue of how to choose the high-dimensional vector of bandwidths or alternatively the kernel covariance matrix. Clearly, cross validation involves an intractable computation cost and plugging in arbitrary values is not recommended, since bandwidth choice fundamentally impacts performance (Liu et al., 2007). Bayesian nonparametric models (Escobar and West, 1995; Rasmussen, 1999) provide an alternative approach for density estimation, specifying priors for the bandwidth parameters allowing adaptive estimation without cross-validation (Shen et al., 2013). However, inference is prohibitively costly. To scale up nonparametric Bayes inference, one can potentially rely on maximum a posteriori (MAP) estimation (Ghahramani et al., 1996) or variational Bayes (VB) (Ghahramani and Beal, 1999). Issues with MAP include difficulties in efficient estimation in high-dimensions, with the EM algorithm tending to converge slowly to a local mode, and lack of characterization of uncertainty. Although VB provides an approximation to the full posterior instead of just the mode, it is well known that posterior uncertainty is substantially underestimated (Wang and Titterington, 2004) and in being implemented with EM, VB inherits the computational problems of MAP estimation.

Manifold learning methods (Tenenbaum et al., 2000; Lawrence, 2005) provide computationally efficient and geometric-oriented dimension reduction, motivating an alternative way to characterize the density via a low-dimensional embedding. While most of these methods have focused on visualization, manifold Parzen windows (Vincent and Bengio, 2003) is a notable exception that has attempted to combine density estimation and manifold learning. The model applies dimension reduction and fits a Gaussian "pancake" to the neighbourhood area of each data point, integrating local geometric information into a kernel density estimator. However, overfitting might come in when every data point is associated, by the same weight, with a Gaussian. Moreover, the model can be sensitive to the prior choice of intrinsic dimension p, and only provides a point estimate. We addressed these problems by designing an empirical Bayes nonparametric density estimator based on a set of multiscale geometric dictionaries learned at a first stage. The proposed estimator combines density estimation and manifold learning, characterizes uncertainty, scales up to problems with massive dimensions and is capable of automatically learning the intrinsic dimension. The

model is illustrated through simulated and real data examples.

The remainder of the paper is organized as follows. Our geometric density estimation (GEODE), consisting of first stage dictionary learning followed by rapid Bayesian inference, is proposed in § 2. The performance of the proposed method is tested through simulation experiments in § 4 and real data applications to image inpainting data handwritten digit classification data in § 5. A discussion is reported in § 6.

2 Bayes dictionary learning in factor models

Assume $\boldsymbol{y}_i \sim \mathcal{N}_D(\boldsymbol{\mu}, \boldsymbol{\Omega})$, with $\boldsymbol{\mu} \in \Re^D$ a mean vector and $\boldsymbol{\Omega} \in \Re^{D\times D}$ a covariance matrix, for $i = 1, 2, \ldots, n$. An efficient approach to reduce dimension when D is large relies on the factor analytic decomposition $\boldsymbol{\Omega} = \boldsymbol{\Lambda}\boldsymbol{\Lambda}^T + \sigma^2\boldsymbol{I}$, where $\boldsymbol{\Lambda}$ is a $D \times p$ matrix with $p \ll D$. Carvalho et al. (2008) and Bhattacharya and Dunson (2011) (among many others) have successfully applied FA under the Bayesian paradigm while additionally assuming $\boldsymbol{\Lambda}$ sparse. The mixture of factor analyzers (MFA) model extends FA to be able to characterize non-Gaussian data. Bayesian MFA is straightforward to implement in small dimensional problems (Diebolt and Robert, 1994; Richardson and Green, 1997), but faces problems in scaling beyond a few 100 dimensions.

To simplify computation, we propose an empirical Bayes approach that avoids directly placing priors on selected parameters in the factorizations via the use of multiscale dictionary learning.

2.1 Formulation

The MFA model is given by

$$f(\boldsymbol{y}_i) \sim \sum_{k=1}^{K} \pi_k \mathcal{N}_D\big(\boldsymbol{\mu}_k, \boldsymbol{\Lambda}_k\boldsymbol{\Lambda}_k^T + \sigma_k^2\boldsymbol{I}\big), \qquad (1)$$

where K is the number of components, $\boldsymbol{\mu}_k \in \Re^D$ is a mean vector and π_k is the mixing weight for the kth component with $\sum_{k=1}^{K}\pi_k = 1$. The intrinsic dimension p is not observable; we start with a guess d with $\boldsymbol{\Lambda}_k$ a $D \times d$ matrix, for $k = 1, \ldots, K$. Later we will discuss how we can efficiently learn p. MFA assumes the data are centered around multiple low–dimensional linear subspaces span($\boldsymbol{\Lambda}_k$), for $k = 1, \ldots, K$. Let $\boldsymbol{\Phi}_k$ be a $D \times d$ matrix with column vectors being the basis for span($\boldsymbol{\Lambda}_k$).

For simplicity, we assume the column vectors of $\boldsymbol{\Phi}_k$ and the column vectors of $\boldsymbol{\Lambda}_k$ are in same directions. Then the MFA model can be written as

$$f(\boldsymbol{y}_i) \sim \sum_{k=1}^{K} \pi_k \mathcal{N}_D\big(\boldsymbol{\mu}_k, \boldsymbol{\Phi}_k\boldsymbol{\Sigma}_k\boldsymbol{\Phi}_k^T + \sigma_k^2\boldsymbol{I}\big), \qquad (2)$$

where $\boldsymbol{\Sigma}_k$ is a $d \times d$ positive diagonal matrix, for $k = 1, \ldots, K$.

If $\boldsymbol{\mu}_k$ and $\boldsymbol{\Phi}_k$ are fixed, the Bayesian learning in high dimensions is clearly greatly simplified, since instead of $\boldsymbol{\Lambda}_k$ and $\boldsymbol{\mu}_k$, only $\boldsymbol{\Sigma}_k$ and σ_k^2, for $k = 1, \ldots, K$, needs to be learned. However, this modification inherits from MFA the problem of choosing K and d, and relies heavily on the quality of the pre–learned dictionaries. To address the problem, we propose a multiscale mixture generalization based on a set of pre–learned multiscale dictionaries $\big\{\boldsymbol{\mu}_{s,h}, \boldsymbol{\Phi}_{s,h}\big\}$ where (s, h) denotes the node index of a binary clustering tree. The dictionaries are obtained in a first stage using geometric multi–resolution analysis (GMRA) (Allard et al., 2012), which is shown to be capable of providing high–quality basis vectors for local linear subspaces at different scales. We call this method the geometric density estimation (GEODE), which can be written as

$$f(\boldsymbol{y}_i) \sim \sum_{s,h} \pi_{s,h} \mathcal{N}_D\big(\boldsymbol{\mu}_{s,h}, \boldsymbol{\Phi}_{s,h}\boldsymbol{\Sigma}_{s,h}\boldsymbol{\Phi}_{s,h}^T + \sigma_s^2\boldsymbol{I}\big), \quad (3)$$

where $\boldsymbol{\Sigma}_{s,h} = \text{diag}(\alpha_{s,h,1}^2, \ldots, \alpha_{s,h,d}^2)$. The proposed method mixes flexibly across a binary tree, both across scales and within scales in a Bayesian manner and hence tends to better capture the nonlinear structure and be more resistant to over–fitting. Moreover, the method is capable of adaptively removing redundant dimensions and efficiently learning the true intrinsic dimension p. Both aspects will be demonstrated in more details later.

Borrowing the notations from Allard et al. (2012), $\boldsymbol{y}_i$, for $i = 1, 2, \ldots, n$, are assumed to have support on $(\mathcal{M}, \mathcal{F}, \mu)$, where $\mathcal{M} \subset \Re^D$, $\mathcal{F}$ is a σ-field defined on $\mathcal{M}$ and μ is a probability measure defined on $\mathcal{F}$. With $s = 0, \ldots, \infty$ denoting the scale index and $h = 1, \ldots, 2^s$ denoting the node index within scale s, the binary clustering tree is defined as follows.

Definition 1. *A **binary clustering tree** of a metric measure space $(\mathcal{M}, \mathcal{F}, \mu)$ is a family of open sets in $\mathcal{M}$, $\{Cell_{s,h}\}$, called dyadic cells, such that*

1. for every s, $\mu(\mathcal{M} \setminus \bigcup_{h=1}^{2^s} Cell_{s,h}) = 0$;

2. for $s \le s'$ and $1 \le h' \le 2^{s'}$, either $Cell_{s',h'} \subseteq Cell_{s,h}$ or $\mu(Cell_{s',h'} \cap Cell_{s,h}) = 0$;

3. for $s < s'$ and $1 \le h' \le 2^{s'}$, there exists a unique $h = 1, 2, \ldots, 2^s$ such that $Cell_{s',h'} \subseteq Cell_{s,h}$.

To learn the multiscale dictionaries, we implement the following three steps:

1. Obtain a binary clustering tree, $Cell_{s,h}$ for $s = 0, \ldots, \infty$ and $h = 1, \ldots, 2^s$ using METIS (Karypis and Kumar, 1998), with the proximity matrix computed using the approximate nearest neighbour (ANN) algorithm (Arya et al., 1998).

2. Estimate a d-dimensional affine approximation in each dyadic cell $Cell_{s,h}$ using fast rank-d SVD (Rokhlin et al., 2009), yielding a local dictionary associated to this cell, denoted $\boldsymbol{\Phi}_{s,h}$.

3. Set $\boldsymbol{\mu}_{s,h}$ equal to the sample mean of $Cell_{s,h}$.

To illustrate these three steps, a 4–level binary clustering tree of a synthetic parabola point cloud obtained using GMRA can be found in the appendix. The likelihood function for the general node (s, h) is

$$f_{s,h}(\boldsymbol{y}_i) = \mathcal{N}_D\big(\boldsymbol{y}_i; \boldsymbol{\mu}_{s,h}, \boldsymbol{\Phi}_{s,h}\boldsymbol{\Sigma}_{s,h}\boldsymbol{\Phi}_{s,h}^T + \sigma_s^2\boldsymbol{I}\big). \quad (4)$$

With basic linear algebra we can write (4) as

$$f_{s,h}(\boldsymbol{y}_i) \propto (\sigma_s^2)^{-D/2} \prod_{m=1}^{d} u_{s,h,m}^{1/2} \exp\Big\{ -\frac{1}{2}\sigma_s^{-2} \times \big[A_{s,h,i} - \sum_{m=1}^{d}(1 - u_{s,h,m})(Z_{s,h,i}^{(m)})^2\big]\Big\}, \quad (5)$$

where $A_{s,h,i} = \tilde{\boldsymbol{y}}_i^T\tilde{\boldsymbol{y}}_i$, $\tilde{\boldsymbol{y}}_i = \boldsymbol{y}_i - \boldsymbol{\mu}_{s,h}$, $u_{s,h,m} = (1 + \sigma_s^{-2}\alpha_{s,h,m}^2)^{-1}$, for $m = 1, \ldots, d$, and $\boldsymbol{Z}_{s,h,i} = \boldsymbol{\Phi}_{s,h}^T\tilde{\boldsymbol{y}}_i$, with $Z_{s,h,i}^{(m)}$ denoting its mth element. Details are reported in the appendix.

We first specify a prior for the "full" model where $d = D$. When p is small, which we expect provides a good approximation in many applications, the information contained in the last $D - p$ columns of $\boldsymbol{\Phi}_{s,h}$ (columns of $\boldsymbol{\Phi}_{s,h}$ are ordered to be descending in their singular values) is negligible and treated as noise. We use a specially tailored prior that shrinks α_m^2 to zero more aggressively as m grows; this reduces MSE by pulling the small signals towards zero. This is equivalent to shrinking u_m increasingly for larger m. To accomplish this adaptive shrinkage, we propose a multiplicative exponential process prior that adapts the prior of Bhattacharya and Dunson (2011), while placing an inverse-gamma prior on σ_s^2, for $s = 0, \ldots, \infty$:

$$\begin{aligned} \sigma_s^{-2} &\sim \mathrm{Ga}(a_\sigma, b_\sigma) \\ u_{s,h,m} &\sim \mathrm{Ga}_{(0,1)}(\delta_{s,h,m} + 1, 1) \\ \delta_{s,h,m} &= \prod_{k=1}^{m} \tau_{s,h,k} \\ \tau_{s,h,k} &\sim \mathrm{Exp}_{[1,\infty)}(a) \end{aligned} \quad (6)$$

where $\tau_{s,h,k}$, for $k = 1, \ldots, d$, are independent truncated exponential random variables, $\delta_{s,h,m}$ and $\tau_{s,h,m}$ are the global and the local shrinkage parameter for the mth column vector of $\boldsymbol{\Phi}_{s,h}$, respectively. Since $\tau_{s,h,k} \geq 1$ for $k = 1, \ldots, D$, $\delta_{s,h,m} = \prod_{k=1}^{m}\tau_{s,h,k}$ is increasing with respect to m. As a result, $u_{s,h,m}$ is stochastically approaching one since the truncated gamma density concentrates around one as $\delta_{s,h,m}$ increases.

However, for large D it is wasteful to conduct computation for the full model, because as m increases $u_{s,h,m}$ is shrunk very strongly to one, and the excess dimensions are effectively discarded. Hence, we propose to truncate the model by setting $u_{s,h,m} = 1$ ($\alpha_{s,h,m}^2 = 0$) for $m > d$, with d an upper bound on the number of factors. The following theorem shows that the approximation error of the truncated prior decreases exponentially in d. The proof is reported in the appendix.

Theorem 1. *Assume $\boldsymbol{\Omega}_{s,h} = \boldsymbol{\Psi}\boldsymbol{\Sigma}_{s,h}\boldsymbol{\Psi}^T + \sigma_s^2\boldsymbol{I}$ where $\boldsymbol{\Psi}$ is a orthonormal $D \times D$ matrix and $\boldsymbol{\Sigma}_{s,h}$ is a $D \times D$ positive diagonal matrix. The distributions of $\boldsymbol{\Sigma}_{s,h}$ and σ_s^2 are defined in (6). Let $\boldsymbol{\Psi}^d$ denote the first d columns of $\boldsymbol{\Psi}$, $\boldsymbol{\Sigma}_{s,h}^d = \mathrm{diag}(\alpha_{s,h,1}^2, \ldots, \alpha_{s,h,d}^2)$ and let $\boldsymbol{\Omega}_{s,h}^d = \boldsymbol{\Psi}^d\boldsymbol{\Sigma}_{s,h}^d\big(\boldsymbol{\Psi}^d\big)^T + \sigma_s^2\boldsymbol{I}$. Then for any $\epsilon > 0$,*

$$Pr\{d_\infty(\boldsymbol{\Omega}_{s,h}, \boldsymbol{\Omega}_{s,h}^d) > \epsilon\} < \frac{6ba^d}{\epsilon(1-a)}$$

for $d > 2\log\{b/\epsilon(1-a)\}/\log(1/a)$, where $d_\infty(\boldsymbol{\Omega}_{s,h}, \boldsymbol{\Omega}_{s,h}^d)$ is defined as $\|\boldsymbol{\Omega}_{s,h} - \boldsymbol{\Omega}_{s,h}^d\|_\infty$. $\|A\|_\infty$ calculates the maximum absolute row sum of the matrix A, $b = E(\sigma_s^2)$ and $a = E(\frac{1}{\tau_{s,h,1}})$.

We then finish the formulation of GEODE by choosing a prior for the multiscale mixing weights $\pi_{s,h}$. This prior should be structured to allow adaptive learning of the appropriate tradeoff between coarse and fine scales. Heavily favoring coarse scales may lead to reduced variance but also high bias if the coarse scale approximation is not accurate. High weights on fine scales may lead to low bias but high variance due to limited sample size in each fine resolution component. With this motivation, Canale and Dunson (2014) proposed a multiresolution stick-breaking process generalizing usual "flat" stick-breaking (Sethuraman, 1994). In particular, let

$$S_{s,h} \sim Be(1, a_S),\ R_{s,h} \sim Be(b_R, b_R) \quad (7)$$

with $S_{s,h}$ denoting the probability that the observation stops at node (s, h) of a binary tree and $R_{s,h}$ denoting the probability that the observation moves down to the right from node (s, h) conditioning on not stopping at node (s, h). Hence

$$\pi_{s,h} = S_{s,h}\prod_{r<s}(1 - S_{r,g_{s,h,r}})T_{s,h,r} \quad (8)$$

where $g_{s,h,r} = \lceil h/2^{s-r} \rceil$ denotes the ancestors of node (s,h) at scale r, $T_{s,h,r} = R_{r,g_{s,h,r}}$ if node $(r+1, g_{s,h,r+1})$ is the right daughter of node$(r+1, g_{s,h,r})$, otherwise $T_{s,h,r} = 1 - R_{r,g_{s,h,r}}$. Canale and Dunson (2014) showed that $\sum_{s=0}^{\infty} \sum_{h=1}^{2^s} \pi_{s,h} = 1$ almost surely for any $a_S, b_R > 0$. This result makes the defined weights a proper set of multiscale mixing weights. As a_S increases, finer scales are favored, resulting in a highly non-Gaussian density.

In practice, it is appealing to approximate the model by a finite-depth multiscale mixture. Let L denote this depth and let $\{\tilde{\pi}_{s,h}\}_{s \le L}$ denote the truncated weights, which are identical to $\{\pi_{s,h}\}$ except that the stopping probabilities at scale L are set to be equal to one to ensure $\sum_{s=1}^{L} \sum_{h=1}^{2^s} \tilde{\pi}_{s,h} = 1$. The accuracy of the approximation is discussed in the following theorem. The proof is reported in the appendix.

Theorem 2. *Let*

$$f^L(\boldsymbol{y}_i) = \sum_{s=1}^{L} \sum_{h=1}^{2^s} \tilde{\pi}_{s,h} \mathcal{N}_D(\boldsymbol{y}_i; \boldsymbol{\mu}_{s,h}, \boldsymbol{\Phi}_{s,h} \boldsymbol{\Sigma}_{s,h} \boldsymbol{\Phi}_{s,h}^T + \sigma_s^2 \boldsymbol{I})$$

denote the approximation at scale L, let $P(B) = \int_B f(\boldsymbol{y}_i) dy$ and $P^L(B) = \int_B f^L(\boldsymbol{y}_i) dy$, for all $B \subset \Re^D$ denote the probability measures corresponding to density $f(\boldsymbol{y}_i)$ and $f^L(\boldsymbol{y}_i)$. Then we have,

$$d_{TV}(P_L, P) < \left(\frac{a_S}{1 + a_S} \right)^L,$$

where $d_{TV}(P_L, P)$ denotes the total variation distance between $P_L(B)$ and $P(B)$.

The above theorem indicates that the approximation error decays at an exponential rate.

2.2 Posterior Computation

The usual frequentist method of selecting an upper-bound d thresholds the singular values, leading to substantial sensitivity to threshold choice. For large D, the upper bound d has to be chosen in advance so that fast rank-d SVD can be achieved (Rokhlin et al., 2009). Typically, conservative choice for d is implemented in order to ensure $d \ge p$, adding a burden to both computation and storage. We avoid this by automatically deleting redundant dictionary elements, and hence decreasing d, as computation proceeds. To this end we adopt an adaptive Gibbs sampler similar to that developed by Bhattacharya and Dunson (2011). The adaptive Gibbs sampler randomly deletes redundant dimensions at tth iteration according to probability $p(t) = \exp(c_0 + c_1 t)$. The values of c_0 and c_1 are chosen to ensure frequent adaption at the beginning of the chain and an exponentially fast decay in frequency after that. We fix $c_0 = -1$, $c_1 = -0.005$ and $tol = 10^{-4}$ as default, where tol is a prespecified threshold.

Introduce the membership variables (s_i, h_i), then the conditional posterior is given by

$$\begin{aligned} p(s_i = s, h_i = h) \propto & \pi_{s,h} \mathcal{N}_D(\boldsymbol{\mu}_{s,h}, \\ & \boldsymbol{\Phi}_{s,h} \boldsymbol{\Sigma}_{s,h} \boldsymbol{\Phi}_{s,h}^T + \sigma_s^2 \boldsymbol{I}). \end{aligned} \tag{9}$$

A multiscale slice sampler (Canale and Dunson, 2014) could save computation when L is large. The conditional posteriors of $S_{s,h}$ and $R_{s,h}$ are given by

$$\begin{aligned} S_{s,h} &\sim \text{Beta}(1 + n_{s,h}, a_S + v_{s,h} - n_{s,h}), \\ R_{s,h} &\sim \text{Beta}(b_R + r_{s,h}, b_R + v_{s,h} - n_{s,h} - r_{s,h}), \end{aligned} \tag{10}$$

where $v_{s,h}$ is the number of observations passing through node (s,h), $n_{s,h}$ is the number of observations stopping at node (s,h), and $r_{s,h}$ is the number of observations that continue to the right after passing through node (s,h). The slice sampler contributes to the computation by allowing the allocation to take place in a subset of all scales of the tree, which can be efficient when we have a deep tree structure. Let $\mathcal{D}_{s,h}$ denote the set of deleted dimension indices (the deleted pool) of node (s,h) and $\mathcal{R}_{s,h}$ denote the set of retained dimension indices (the remaining pool) of node (s,h). Combining all the techniques discussed above, the Bayesian GEODE algorithm can be summarized as follows

The first stage:

1. Compute a multiscale dictionary $\{\boldsymbol{\Phi}_{s,h}, \boldsymbol{\mu}_{s,h}\}$ using GMRA and initialize the algorithm.

The second stage, iterate until the desired posterior sample size:

1. Update s_i and h_i for all i according to (9).
2. Update $S_{s,h}$ and $R_{s,h}$ for all s and h according to (10).
3. Update $u_{s,h,m}$ for all s, h and m according to $\text{Gamma}_{(0,1)}(\hat{a}_{s,h,m}, \hat{b}_{s,h,m})$, where $\hat{a}_{s,h,m} = \prod_{k=1}^{m} \tau_{s,h,k} + n_{s,h}/2$ and $\hat{b}_{s,h,m} = 1 + \frac{1}{2}\sigma_s^{-2} \sum_{y_i \in C_{s,h}} (\boldsymbol{Z}_{s,h,i}^{(m)})^2$.
4. Update $\tau_{s,h,m}$ for all s, h and m according to $\text{Exp}_{[1,\infty)}(\hat{\lambda}_{s,h,m})$, where $\hat{\lambda}_{s,h,m} = a_\tau - \ln(\prod_{j>m-1} u_{s,h,j})$
5. Update σ_s^{-2} for all s according to $\text{Gamma}(\hat{c}_s, \hat{d}_s)$, where $\hat{c}_s = a_\sigma + Dn_s/2$, $\hat{d}_s = \frac{1}{2} \sum_{y_i \in C_s} \left[A_{s,h,i} - \sum_{j=1}^{d} (1 - u_{s,h,j}) (\boldsymbol{Z}_{s,h,i}^{(j)})^2 \right] + b_\sigma$, C_s denotes the set of observations stopping at scale s, and n_s denotes the size of C_s.

6. Compute $p(t) = \exp(c_0 + c_1 t)$, generate g from Uniform$(0,1)$. If $g > p(t)$, go back to step 2 until the desired iteration number.

7. For all (s,h), compute $r^t_{s,h,m} = \left(\alpha^t_{s,h,m}\right)^2 / \max_{j\in\mathcal{R}_{s,h}} \left(\alpha^t_{shj}\right)^2$, for $m \in \mathcal{R}_{s,h}$. Remove all m from $\mathcal{R}_{s,h}$ to $\mathcal{D}_{s,h}$ if $r^t_{s,h,m} < tol$. If no such m exists, then randomly add back one dimension m from $\mathcal{D}_{s,h}$ to $\mathcal{R}_{s,h}$ according to $p(m) \propto I_{m\in\mathcal{D}_{s,h}} r^{t-1}_{s,h,m}$.

The derivation of all the conditional posteriors can be found in the supplement. Through the paper, we fix $a_\sigma = 1/2$, $b_\sigma = 1/2$ and $a = 0.05$, and use the default parameters in the GMRA code provided by Allard et al. (2012).

2.3 Missing Data Imputation

Bayesian models better utilize the partially observed data by probabilistically imputing the missing features based on its conditional posterior distribution. Notations $\boldsymbol{y}_M$ and $\boldsymbol{y}_O$ are introduced as the missing part and the observed part of $\boldsymbol{y}$ respectively. Similarly, slightly abusing the notations, let $\boldsymbol{\mu}_M$ and $\boldsymbol{\Phi}_M$ denote the missing parts of $\boldsymbol{\mu}_{s,h}$ and $\boldsymbol{\Phi}_{s,h}$, and let $\boldsymbol{\mu}_O$ and $\boldsymbol{\Phi}_O$ denote the observed parts. The following proposition enables efficient sampling from the conditional posterior distribution $p(\boldsymbol{y}_M|\boldsymbol{y}_O, \boldsymbol{\Theta})$, where $\boldsymbol{\Theta}$ denotes the all unknown parameters in the model. The computational analysis is provided in § 3 and simulation studies are provided in § 4.

Proposition 1. *For node (s,h), introduce augmented data $\boldsymbol{\eta}_i$ such that $(\boldsymbol{y}_i|\boldsymbol{\eta}_i, \boldsymbol{\Theta}, s_i = s, h_i = h) \sim \mathcal{N}_D(\boldsymbol{\mu}_{s,h} + \boldsymbol{\Phi}_{s,h}\boldsymbol{\eta}_i, \sigma_s^2 \boldsymbol{I}_D)$ and $(\boldsymbol{\eta}_i|\boldsymbol{\Theta}, s_i = s, h_i = h) \sim \mathcal{N}_d(0, \boldsymbol{\Sigma}_{s,h})$, for $i = 1, \ldots, n$. Then we have the conditional distribution with $\boldsymbol{\eta}_i$ marginalized out equal $(\boldsymbol{y}_i|\boldsymbol{\Theta}, s_i = s, h_i = h) \sim \mathcal{N}_D(\boldsymbol{\mu}_{s,h} + \boldsymbol{\Phi}_{s,h}\boldsymbol{\Sigma}_{s,h}\boldsymbol{\Phi}^T_{s,h}, \sigma_s^2 \boldsymbol{I}_D)$. Furthermore, conditional on $s_i = s$ and $h_i = h$ we have*

$$\boldsymbol{\eta}_i|\boldsymbol{y}_O, \boldsymbol{\Theta} \sim \mathcal{N}_d(\hat{\boldsymbol{\mu}}_\eta, \hat{\boldsymbol{\Sigma}}_\eta),$$
$$\boldsymbol{y}_M|\boldsymbol{\eta}_i, \boldsymbol{y}_O, \boldsymbol{\Theta} \sim \mathcal{N}_{m_i}(\boldsymbol{\mu}_M + \boldsymbol{\Phi}_M\boldsymbol{\eta}_i, \sigma_s^2 I_{m_i}),$$

where $\hat{\boldsymbol{\Sigma}}_\eta = \left(\boldsymbol{\Sigma}_{s,h}\boldsymbol{\Phi}^T_O\boldsymbol{\Phi}_O/\sigma_s^2 + I\right)^{-1}\boldsymbol{\Sigma}_{s,h}$ and $\hat{\boldsymbol{\mu}}_\eta = \hat{\boldsymbol{\Sigma}}_\eta\boldsymbol{\Phi}^T_O(\boldsymbol{y}_O - \boldsymbol{\mu}_O)/\sigma_s^2$.

The proposition also provides an efficient way to predict multivariate response, which is applied to image inpainting in § 5.1. Proof is reported in the appendix.

3 Computational Aspects

When data are complete, the computational cost of our implementation of GMRA is $O\big(nD(\log n + d^2)\big)$ (Allard et al., 2012). The cost of computing the sufficient statistics $\{A_{s,h,i}\}$, $\{Z_{s,h,i}\}$ is $O\big(nD2^L d\big)$. Hence the overall cost of the first stage is given by

$$O\bigg(nD(\log n + d^2 + 2^L d)\bigg),$$

which only increases linearly in D. Letting T be the total iteration number of the Gibbs sampler, the overall computational cost of the second stage is given by

$$O\bigg(T(2^L d^3 + nd)\bigg),$$

which is independent of D.

When data has missing features, with $\boldsymbol{\Phi}^T_O\boldsymbol{\Phi}_O$ and $\boldsymbol{\Phi}^T_O(\boldsymbol{y}^O_i - \boldsymbol{\mu}_O)$ stored as sufficient statistics, the computational cost of the first stage is given by

$$O\bigg(nD(\log n + d^2 + 2^L d) + n_m D d^2\bigg),$$

and the cost of the second stage is given by

$$O\bigg(T(2^L d^3 + nd + n_m M)\bigg),$$

where n_m denotes the number of partial observations and $M = \max_{i=1,\ldots,n} m_i$.

The computation time of the complete case is reported in Figure 1, where 100 random samples were generated by projecting a 3-D Swissroll into higher dimensional ambient spaces. d was set to be 10. The linearity in the first stage and the independence in the second stage with respect to D can be easily seen.

Differently from GEODE, traditional Bayesian MFA models have to learn and store the $D \times d$ factor loading

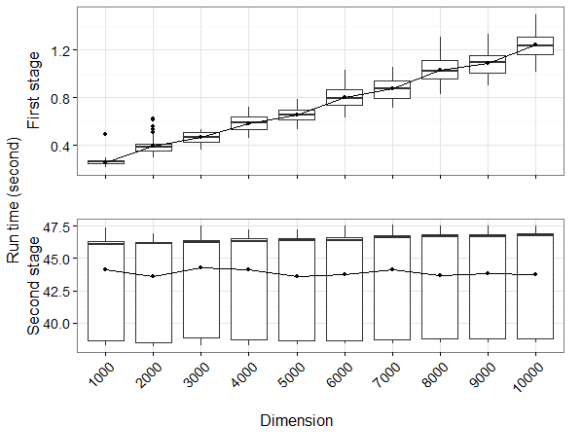

Figure 1: Boxplot of the computational times of 100 replicate experiments at different ambient dimensions, with means jointed by segments.

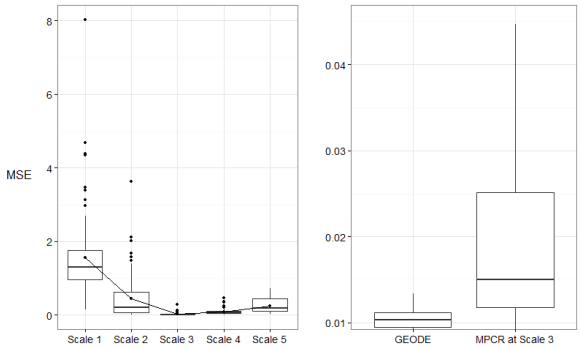

Figure 2: **Left**: Boxplot of predictive MSE of MPCR at different scales; **Right**: Predictive MSE of GEODE compared with the best MPCR can do.

matrices within each iteration in the MCMC, making both the computation and the storage daunting tasks when D is very large. Moreover, due to the reduced number of parameters and lower posterior dependence in these parameters, our Gibbs sampler for GEODE converges and mixes dramatically faster than MCMC algorithms for fully Bayesian MFA models. This reduces the number of samples needed; we run the sampler 1,000 iterations, with the first 500 as a burn-in. Experimental results show convergence typically occurs very fast.

Note that all data experiments in the paper were run in matlab version 2012a on a x86_64 linux machine with a 8×3.40 GHz Intel(R) Core(TM) i7-3770 processor. Furthermore, note that our Gibbs sampler is written in matlab and hence the computing time of the second stage could be greatly reduced using lower level languages.

4 Simulation Studies

To demonstrate GEODE, several simulation studies were conducted. Our aim is to highlight several characteristics of the approach: the improved quality by mixing over different scales, the ability to learn the true intrinsic dimension or a tight upperbound, the ability to impute missing data and the accurate characterization of uncertainty. Through the simulation studies, d was set to be 10, providing an upper bound on the intrinsic dimension. The method is not sensitive to the choice of this upper bound.

4.1 Smoothness Adaptation

By mixing across different scales, GEODE is able to tradeoff between coarser scales and finer scales in a Bayesian manner adapting to the local smoothness. To see this, a multi-scale principal component regression (MPCR) based on GMRA is proposed and compared with GEODE. The MPCR, being a natural combination of GMRA and principal component regression (PCR), learns local regression coefficients by applying PCR to subsets of observations at each node within a specific level. The prediction is made by first assigning the data point to the node closest to this data point in terms of Euclidean distance to the center, and then predicting using the local regression coefficients. It is a natural comparison to GEODE since both use the same binary tree structure and the same multiscale dictionaries. MPCR predicts based on all the nodes within a specific scale while GEODE mixes over all scales.

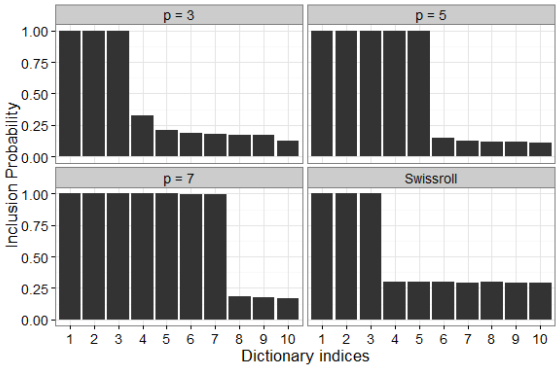

Figure 3: Average inclusion probabilities for each dimension under different scenarios, with 10 being an upper bound.

In the simulation study, 100 independent samples with 1100 observations were generated from a mixture of three Gaussians with $D = 10000$, whose intrinsic dimensions equal 3, 5 and 7 respectively. In each sample, 1000 observations were randomly selected to train the model, and the other 100 were used as test data. One dimension of the test data is assumed to be missing and to be predicted. Performance of GEODE is compared with that of MPCR in terms of the mean square prediction error, which is shown in Figure 2. The MSE curve of MPCR is u-shaped, indicating overfitting at fine scale. MDLR clearly outperforms MPCR even under ideal conditions for MPCR. This suggests that GEODE efficiently utilized the local smoothness information , while adaptively borrowing information across scales.

4.2 Intrinsic Dimension Learning

The adaptive Gibbs sampler automatically excludes unnecessary dimensions. The posterior mean inclusion probabilities are useful in estimating the true intrinsic dimension. These probabilities were computed un-

der each simulation case, with results shown in Figure 3. In the Gaussian mixture case, GEODE successfully learned the true p, with the redundant dimensions excluded with more than 70% probability, saving computation and storage. For the Swissroll example, GEODE instead provided a tight upperbound for the true p.

4.3 Regression With Missing Data

In this simulation study, 100 independent samples are generated from 9 different scenarios involving Gaussian or manifold (Swissroll) data, different ambient dimensions D and different intrinsic dimensions p. GEODE was compared with competing methods in regression problems either with or without missing data. Scenarios 1 - 6 are linear Gaussian data and scenarios 7-9 are Swissroll data embedded in high dimensional ambient spaces. Simulation details are reported in the appendix.

For Gaussian data, our method is compared with elastic net (EN) and PCR. For Swissroll data, our method is compared with random forest (RF). To make the computation of PCR and RF feasible for our studies, fast rank-k SVD was applied in both cases. RF was applied after the data have been projected to a 10 dimensional space using fast SVD. As can be seen from Figure 5, GEODE has a consistently better predictive accuracy than the competing methods. Moreover, GEODE successfully imputed the missing data while maintaining similar MSE in the presence of missing data, while methods that discard observations with missing data have clearly increased MSE. Empirical 95% coverages of intervals out of sample are presented in Figure 4. As can be seen, GEODE only slightly underestimated uncertainty.

The results demonstrated the capability of the proposed method to properly characterize uncertainty and impute missing data, while maintaining computational efficiency and accurate predictions.

5 Application

GEODE is further demonstrated first in a multivariate response regression application and then in a supervised classification problem. In both applications, $d = 20$. Increasing d moderately had essentially no impact on the results.

5.1 Image Inpainting

The Frey faces data (Roweis et al., 2002) contains 1965 20×28 video frames of a single face with different expressions. Conducting the same experiment as done by

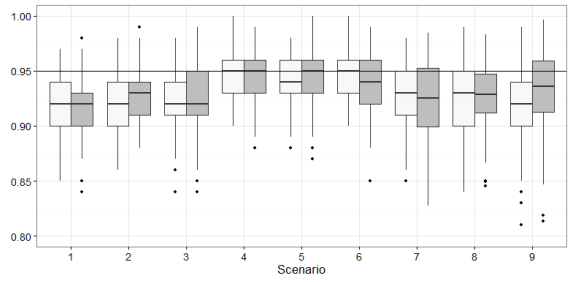

Figure 4: Boxplots of the empirical coverages of 100 replicate experiments, with fully observed datasets denoted by light grey and partially observed ones denoted by dark grey.

Titsias and Lawrence (2010), the data set is randomly split into 1000 training images and 965 testing images with a random half of the pixels missing. GEODE was trained for less than 2 minutes, and reconstruction (prediction) of all 965 testing images was done in less than 10 minutes. The mean absolute reconstruction error of GEODE is 7.04, which outperforms the error of 7.40 reported by Titsias and Lawrence (2010). 10 randomly selected reconstructions are shown on the left in Figure 6, with 4 manually designed missingness cases shown on the right. GEODE also outperforms the results shown by Adams et al. (2010) by looking at their visualized results. It is also noted that Adams et al. (2010) reported a few hours of computational time in reconstructing 100 images based on 1865 training images.

5.2 Digit Classification

GEODE was used as a probabilistic classifier for the MNIST handwritten data, which contains 70000 28×28 grey scale handwritten digits images. First, one GEODE was trained for each of the 10 digits over a total of 60000 training data for around 90 minutes. Then within each iteration of the Gibbs sampler, the 10 GEODE's worked in a Naive Bayes way and generated a likely class. The "voting" process took 7 minutes for 10000 testing images and the mode of these votes were computed as the classification results. The classification error was 2.32%.

6 Discussion

In many applications, high-dimensional data with unknown joint distribution are collected. Despite the dramatic importance of learning the joint distribution of such data, few probabilistic methods that scale well to high-dimension and provide an adequate characterization of uncertainty are available. Bayesian non-

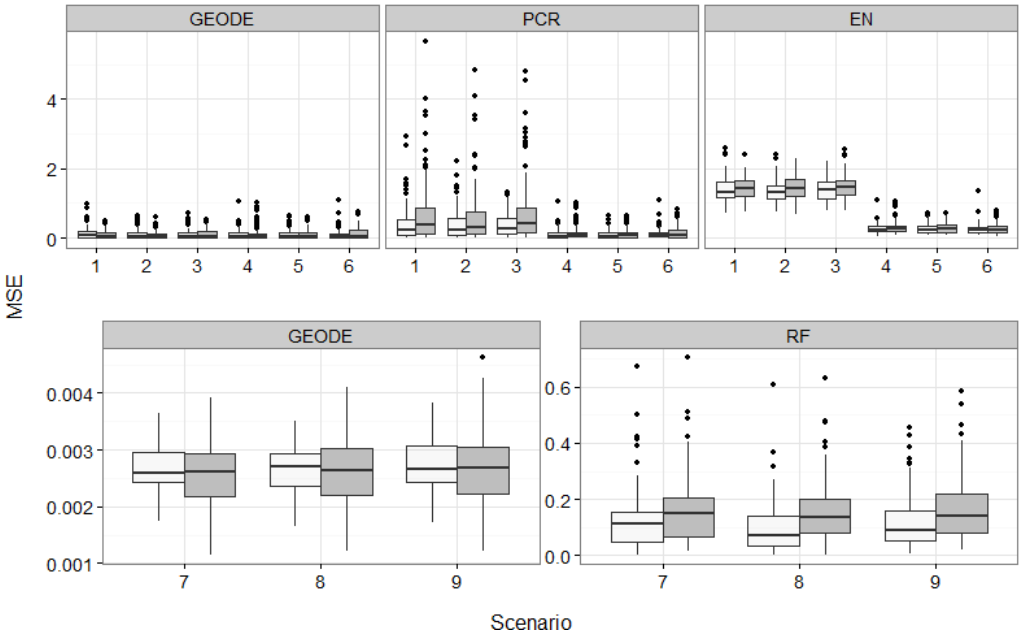

Figure 5: Comparison of performance between GEODE and other methods with respect to MSE, the vertical bars represent the 95% empirical intervals, with fully observed datasets denoted by light grey and partially observed ones denoted by dark grey.

Figure 6: The first row shows the original images, second row shows the images with pixels missing, and the third row shows the reconstructed images.

parametric methods based on mixtures of multivariate Gaussian kernels are widely used, but face major bottlenecks in scaling to higher dimensions. To tackle this problem, we proposed an empirical Bayes density estimator combining manifold learning and Bayesian nonparametric density estimation. One of the building blocks of our method focuses on single Gaussian factor decomposition in which variables are linearly related, showing excellent performance in scaling computationally and in generalization error, while providing a valid characterization of uncertainty in predictions. The other building block is a multiscale mixture generalization, which accommodates unknown density, nonlinear relationships and nonlinear subspaces. This approach showed excellent performance in inferring the subspace dimension, estimating the subspace, and characterizing the joint density of the data in the ambient space. The proposed methods are broadly applicable to many learning problems including regression or classification with missing features.

References

R. P. Adams, H. M. Wallach, and Z. Ghahramani. Learning the structure of deep sparse graphical models. *Journal of Machine Learning Research: Workshop and Conference Proceedings (AISTATS)*, 9:1–8, 05/2010 2010.

W. K. Allard, G. Chen, and M. Maggioni. Multi-scale geometric methods for data sets ii: Geometric multi-resolution analysis. *Applied and Computational Harmonic Analysis*, 32(3):435–462, 2012.

S. Arya, D. M. Mount, N. S. Netanyahu, R. Silverman, and A. Y. Wu. An optimal algorithm for approxi-

mate nearest neighbor searching fixed dimensions. *Journal of the ACM (JACM)*, 45(6):891–923, 1998.

A. Bhattacharya and D. B. Dunson. Sparse Bayesian infinite factor models. *Biometrika*, 98(2):291–306, 2011.

A. Canale and D. B. Dunson. Multiscale Bernstein polynomials for densities. 2014. `arXiv:1410.0827 [stat.ME]`.

C. M. Carvalho, J. Chang, J. E. Lucas, J. R. Nevins, Q. Wang, and M. West. High-dimensional sparse factor modeling: applications in gene expression genomics. *Journal of the American Statistical Association*, 103(484), 2008.

J. Diebolt and C. P. Robert. Estimation of finite mixture distributions through bayesian sampling. *Journal of the Royal Statistical Society. Series B (Statistical Methodology)*, 56(2):363–375, 1994.

M. D. Escobar and M. West. Bayesian density estimation and inference using mixtures. *Journal of the American Statistical Association*, 90(430):577–588, 1995.

Z. Ghahramani and M. J. Beal. Variational inference for Bayesian mixtures of factor analysers. In *NIPS*, volume 12, pages 449–455, 1999.

Z. Ghahramani, G. E. Hinton, et al. The EM algorithm for mixtures of factor analyzers. Technical report, CRG-TR-96-1, University of Toronto, 1996.

G. Karypis and V. Kumar. A fast and high quality multilevel scheme for partitioning irregular graphs. *SIAM Journal on Scientific Computing*, 20(1):359–392, 1998.

N. Lawrence. Probabilistic non-linear principal component analysis with Gaussian process latent variable models. *The Journal of Machine Learning Research*, 6:1783–1816, 2005.

H. Liu, J. D. Lafferty, and L. A. Wasserman. Sparse nonparametric density estimation in high dimensions using the rodeo. In *International Conference on Artificial Intelligence and Statistics*, pages 283–290, 2007.

C. E. Rasmussen. The infinite Gaussian mixture model. In *NIPS*, volume 12, pages 554–560. MIT; 1998, 1999.

S. Richardson and P. J. Green. On Bayesian analysis of mixtures with an unknown number of components (with discussion). *Journal of the Royal Statistical Society: Series B (Statistical Methodology)*, 59(4): 731–792, 1997.

V. Rokhlin, A. Szlam, and M. Tygert. A randomized algorithm for principal component analysis. *SIAM Journal on Matrix Analysis and Applications*, 31(3): 1100–1124, 2009.

S. T. Roweis, L. K. Saul, and G. E. Hinton. Global coordination of local linear models. In *NIPS*, volume 2, pages 889–896. MIT; 1998, 2002.

J. Sethuraman. A constructive definition of Dirichlet priors. *Statistica Sinica*, 4:639–650, 1994.

W. Shen, S. T. Tokdar, and S. Ghosal. Adaptive Bayesian multivariate density estimation with Dirichlet mixtures. *Biometrika*, 100(4):623–640, 2013.

J. B. Tenenbaum, V. De Silva, and J. C. Langford. A global geometric framework for nonlinear dimensionality reduction. *Science*, 290(5500):2319–2323, 2000.

M. Titsias and N. Lawrence. Bayesian Gaussian process latent variable model. In *the International Conference on Articial Intelligence and Statistics*, 2010.

P. Vincent and Y. Bengio. Manifold parzen windows. In *NIPS*, volume 15, pages 849–856. MIT; 1998, 2003.

B. Wang and M. Titterington. Inadequacy of interval estimates corresponding to variational Bayesian approximations. In *10th Int. Workshop Artific. Intell. Statist. Ed. R.G. Cowell*, 2004.

Appendix

A Formulation

To illustrate the binary clustering tree, a 4–level binary clustering tree of a synthetic parabola point cloud obtained using GMRA can be found in Figure 7.

The likelihood function of GEODE can be written as

$$f_{s,h}(\boldsymbol{y}_i) \propto (\sigma_s^2)^{-D/2} \prod_{m=1}^{d} u_{s,h,m}^{1/2} \times \exp\Big\{ -\frac{1}{2}\sigma_s^{-2} \big[A_{s,h,i} - \sum_{m=1}^{d}(1-u_{s,h,m})(Z_{s,h,i}^{(m)})^2\big]\Big\}, \tag{A1}$$

which can be derived using the following two propositions.

Proposition 2. *$\boldsymbol{\Sigma} = diag(\alpha_1^2, \ldots, \alpha_d^2)$ is a $d \times d$ matrix with all diagonal entries larger than 0, $\boldsymbol{\Phi}$ is a $D \times d$ orthonormal matrix, we have,*

$$(\sigma^2 \boldsymbol{I} + \boldsymbol{\Phi}\boldsymbol{\Sigma}\boldsymbol{\Phi}^T) = \sigma^{-2}\boldsymbol{I} - \sigma^{-4}\boldsymbol{\Phi}\tilde{\boldsymbol{\Sigma}}\boldsymbol{\Phi}^T,$$

where $\tilde{\boldsymbol{\Sigma}} = diag(\frac{\alpha_1^2}{1+\sigma^{-2}\alpha_1^2}, \frac{\alpha_2^2}{1+\sigma^{-2}\alpha_2^2}, \ldots, \frac{\alpha_d^2}{1+\sigma^{-2}\alpha_d^2})$.

Proof. By the orthonormality of the dictionary, we have $\boldsymbol{\Phi}^T\boldsymbol{\Phi} = \boldsymbol{I}_d$. And by the matrix inversion formula,

$$\begin{aligned}(\sigma^2 I + \boldsymbol{\Phi}\boldsymbol{\Sigma}\boldsymbol{\Phi}^T)^{-1} &= \sigma^{-2}\boldsymbol{I} - \sigma^{-4}\boldsymbol{\Phi}(\boldsymbol{I} + \sigma^{-2}\boldsymbol{\Sigma}\boldsymbol{\Phi}^T\boldsymbol{\Phi})^{-1}\boldsymbol{\Sigma}\boldsymbol{\Phi}^T \\ &= \sigma^{-2}\boldsymbol{I} - \sigma^{-4}\boldsymbol{\Phi}(\boldsymbol{I} + \sigma^{-2}\boldsymbol{\Sigma})^{-1}\boldsymbol{\Sigma}\boldsymbol{\Phi}^T \\ &= \sigma^{-2}\boldsymbol{I} - \sigma^{-4}\boldsymbol{\Phi}\tilde{\boldsymbol{\Sigma}}\boldsymbol{\Phi}^T\end{aligned}$$

□

Proposition 3. *Under the same setting of Proposition 2, we have*

$$|\sigma^2\boldsymbol{I} + \boldsymbol{\Phi}\boldsymbol{\Sigma}\boldsymbol{\Phi}^T|^{-1/2} = (\sigma^2)^{-D/2}\prod_{m=1}^{d}(\frac{1}{1+\sigma^{-2}\alpha_m^2})^{1/2}.$$

Proof. By Theorem Schur's formula,

$$\begin{aligned}|\sigma^2\boldsymbol{I} + \boldsymbol{\Phi}\boldsymbol{\Sigma}\boldsymbol{\Phi}^T|^{-1/2} &= (\sigma^2)^{-D/2}|\boldsymbol{I}_D + \sigma^{-2}\boldsymbol{\Phi}\boldsymbol{\Sigma}\boldsymbol{\Phi}^T|^{-1/2} \\ &= (\sigma^2)^{-D/2}|\boldsymbol{I}_d + \sigma^{-2}\boldsymbol{\Sigma}^{1/2}\boldsymbol{\Phi}^T\boldsymbol{\Phi}\boldsymbol{\Sigma}^{1/2}|^{-1/2} \\ &= (\sigma^2)^{-D/2}|\boldsymbol{I}_d + \sigma^{-2}\boldsymbol{\Sigma}| \\ &= (\sigma^2)^{-D/2}\prod_{m=1}^{d}(\frac{1}{1+\sigma^{-2}\alpha_m^2})^{1/2}\end{aligned}$$

□

Theorem 3. *Assume $\boldsymbol{\Omega}_{s,h} = \boldsymbol{\Psi}\boldsymbol{\Sigma}_{s,h}\boldsymbol{\Psi}^T + \sigma_s^2\boldsymbol{I}$ where $\boldsymbol{\Psi}$ is a orthonormal $D \times D$ matrix and $\boldsymbol{\Sigma}_{s,h}$ is a $D \times D$ positive diagonal matrix. The distributions of $\boldsymbol{\Sigma}_{s,h}$ and σ_s^2 are defined in (6) and (7) in the submitted paper. Let $\boldsymbol{\Psi}^d$ denote the first d columns of $\boldsymbol{\Psi}$, $\boldsymbol{\Sigma}_{s,h}^d = \mathrm{diag}(\alpha_{s,h,1}^2, \ldots, \alpha_{s,h,d}^2)$ and let $\boldsymbol{\Omega}_{s,h}^d = \boldsymbol{\Psi}^d\boldsymbol{\Sigma}_{s,h}^d(\boldsymbol{\Psi}^d)^T + \sigma_s^2\boldsymbol{I}$. Then for any $\epsilon > 0$,*

$$Pr\{d_\infty(\boldsymbol{\Omega}_{s,h}, \boldsymbol{\Omega}_{s,h}^d) > \epsilon\} < \frac{6ba^d}{\epsilon(1-a)}$$

for $d > 2\log\{b/\epsilon(1-a)\}/\log(1/a)$, where $d_\infty(\boldsymbol{\Omega}_{s,h}, \boldsymbol{\Omega}_{s,h}^d)$ is defined as $\|\boldsymbol{\Omega}_{s,h} - \boldsymbol{\Omega}_{s,h}^d\|_\infty$. $\|A\|_\infty$ calculates the maximum absolute row sum of the matrix A, $b = E(\sigma_s^2)$ and $a = E(\frac{1}{\tau_{s,h,1}})$.

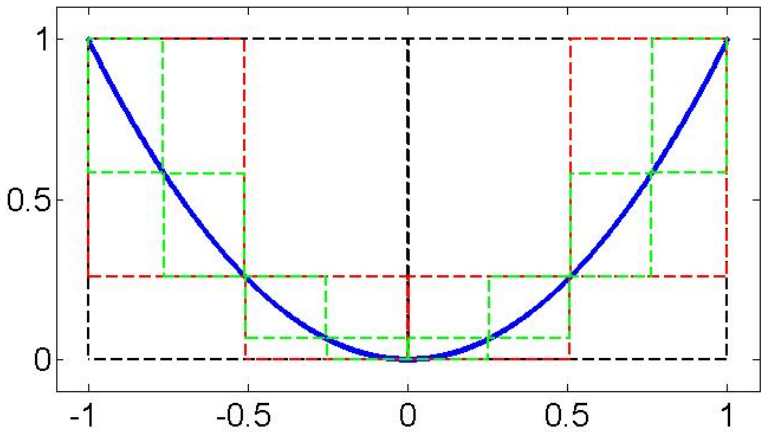

Figure 7: A 4 level binary tree decomposition of a parabola using METIS, with the black rectangular denoting the second level cells, the red denoting the third level cells and the green denoting the leaf cells.

Proof. With a slight abuse of notation, we write $u_{s,h,k}$ as u and let $A = \prod_{m=1}^{K} \tau_{s,h,m}$. Let $\triangle_d = \mathbf{\Psi}\mathbf{\Sigma}_{s,h}\mathbf{\Psi}^T - \mathbf{\Psi}^d\mathbf{\Sigma}^d_{s,h}(\mathbf{\Psi}^d)^T$, $\triangle_d = \{a_{i.j}\}$ and $\mathbf{\Psi} = \{\psi_{i,j}\}$. Clearly, $d_\infty(\mathbf{\Omega}_{s,h}, \mathbf{\Omega}^d_{s,h}) = \max_{1\le i,j\le D} |a^d_{i,j}|$, and $a^d_{i,j} = \sum_{k=d+1}^{D} \alpha_k^2 \psi_{i,k}\psi_{j,k}$. By Cauchy-Schwartz inequality,

$$|\sum_{k=d+1}^{D} \alpha_k^2 \psi_{i,k}\psi_{j,k}| \le \max_{1\le m\le D}(\sum_{k=H+1}^{D} \alpha_k^2 \psi_{m,k}^2).$$

Since $\mathbf{\Psi}$ is orthonormal, we have $\psi_{i,j}^2 \le 1$ for any i and j. Hence

$$d_\infty(\mathbf{\Omega}_{s,h}, \mathbf{\Omega}^d_{s,h}) \le \sum_{k=d+1}^{D} \alpha_k^2.$$

For a fixed $\epsilon > 0$, by Chebyshev's inequalities

$$\begin{aligned} p\{d_\infty(\mathbf{\Omega}_{s,h}, \mathbf{\Omega}^d_{s,h}) \le \epsilon\} &\ge p\Big\{\sum_{k=d+1}^{D} \alpha_k^2 \le \epsilon\Big\} \\ &= E\Big\{p(\sum_{k=d+1}^{D} \alpha_k^2 \le \epsilon|\tau)\Big\} \\ &= 1 - E\Big\{p(\sum_{k=d+1}^{D} \alpha_k^2 > \epsilon|\tau)\Big\} \\ &\ge 1 - E\Big\{\frac{E(\sum_{k=d+1}^{D} \alpha_k^2|\tau)}{\epsilon}\Big\}. \end{aligned}$$

By design we have $u \sim \mathrm{Ga}_{(0,1)}(A+1, 1)$ and u and σ_s^2 are conditionally independent, hence

$$E[(\frac{1}{u} - 1)\sigma_s^2|\tau] = E[(\frac{1}{u} - 1)|\tau]E(\sigma_s^2).$$

Then we have

$$\begin{aligned} E[(\frac{1}{u}-1)|\tau] &= \frac{\int_0^1 (1/u-1)\frac{u^A}{\Gamma(A+1)}e^{-u}\mathrm{d}u}{\int_0^1 \frac{u^A}{\Gamma(A+1)}e^{-u}\mathrm{d}u} = \frac{\int_0^1 1/u \times u^A e^{-u}\mathrm{d}u}{\int_0^1 u^A e^{-u}\mathrm{d}u} - 1 \\ &= \frac{\int_0^1 u^{A-1}e^{-u}\mathrm{d}u}{\int_0^1 u^A e^{-u}\mathrm{d}u} - 1 = \frac{\frac{1}{A}u^A e^{-u}|_0^1 + \int_0^1 \frac{1}{A}u^A e^{-u}\mathrm{d}u}{\int_0^1 u^A e^{-u}\mathrm{d}u} - 1 \\ &= \frac{e^{-1}}{A\int_0^1 u^A e^{-u}\mathrm{d}u} - 1 + \frac{1}{A}. \end{aligned}$$

Let $\gamma(s,x) = \int_0^x t^{s-1}e^{-t}\mathrm{d}t$ be the lower incomplete Gamma function. Note that,

$$\begin{aligned} A\gamma(A+1,1) &= \frac{A}{A+1}u^{A+1}e^{-u}|_0^1 + \frac{A}{A+1}\gamma(A+2,1) \\ &= \frac{A}{A+1}e^{-1} + \frac{A}{A+1}\left[\frac{1}{A+2}e^{-1} + \frac{1}{A+2}\gamma(A+3,1)\right] \\ &= \lim_{K\to\infty}\left\{\sum_{k=1}^{K}\frac{\Gamma(A+1)^2}{\Gamma(A)\Gamma(A+k+1)}e^{-1} + A\Gamma(A+1)F(1;A+K,1)\right\} \\ &= \sum_{k=1}^{\infty}\frac{\Gamma(A+1)^2}{\Gamma(A)\Gamma(A+k+1)}e^{-1} \\ &= \sum_{k=1}^{\infty}\frac{A}{(A+1)(A+2)\ldots(A+k)}e^{-1} \end{aligned}$$

where $F(x;a,b)$ is the cdf of $\mathrm{Ga}(a,b)$ and $\lim_{a=\infty}F(1;a,1)=0$. Furthermore we have

$$\sum_{k=1}^{\infty}\frac{\Gamma(A+1)^2}{\Gamma(A)\Gamma(A+k+1)} = \textstyle\sum_{k=1}^{\infty}\frac{A}{(A+1)(A+2)\ldots(A+k)} \geq 1/2,$$

and

$$1-\sum_{k=1}^{\infty}\frac{\Gamma(A+1)^2}{\Gamma(A)\Gamma(A+k+1)} \leq 1-\tfrac{A}{A+1} \leq \frac{1}{A},$$

thus we have

$$\begin{aligned} \frac{e^{-1}}{A\int_0^1 u_{s,h,k}^A e^{-u_h}\mathrm{d}u_{s,h,k}} - 1 + \frac{1}{A} &= \frac{1}{\sum_{k=1}^{\infty}\frac{\Gamma(A+1)^2}{\Gamma(A)\Gamma(A+k+1)}} - 1 + \frac{1}{A} \\ &= \frac{1-\sum_{k=1}^{\infty}\frac{\Gamma(A+1)^2}{\Gamma(A)\Gamma(A+k+1)}}{\sum_{k=1}^{\infty}\frac{\Gamma(A+1)^2}{\Gamma(A)\Gamma(A+k+1)}} + \frac{1}{A} \\ &\leq \frac{1/A}{1/2} + \frac{1}{A} \\ &= \frac{3}{A}. \end{aligned}$$

Hence $E[(\frac{1}{u}-1)|\tau] \leq 3/(\prod_{m=1}^{k}\tau_{s,h,m})$. Based on this inequality, we have

$$\begin{aligned} \sum_{k=d+1}^{D} E\Big\{E[(\frac{1}{u}-1)\sigma_s^2|\tau]\Big\} &\leq \textstyle\sum_{k=d+1}^{D} E\left(\frac{3}{\prod_{m=1}^{k}\tau_{s,h,m}}\right)E(\sigma_s^2) \\ &= \textstyle\sum_{k=d+1}^{D} 3ba^k \leq \frac{3ba^d}{1-a} \end{aligned}$$

where $b = E(\sigma_s^2)$ and a $= E(\frac{1}{\tau_{s,h,1}})$. Note that $\tau_{s,h,m} \sim \text{Exp}_{[1,\infty)}(\lambda)$, thus $a < 1$. By Fubini's theorem, $E\Big\{E(\sum_{k=H+1}^{\infty}\alpha_k^2|\tau)\Big\} = \sum_{k=d+1}^{\infty} E\Big\{E[(\frac{1}{u_{s,h,k}}-1)\sigma_s^2|\tau]\Big\}$. Now use inequality $(1-x/2) > \exp(-x)$ if $0 < x \leq 1.5$ to get

$$p\{d_\infty(\boldsymbol{\Omega}_{s,h}, \boldsymbol{\Omega}_{s,h}^d) \leq \epsilon\} \geq \exp\{\frac{-6ba^d}{\epsilon(1-a)}\}$$

if $d > 2\log\{b/\epsilon(1-a)\}/\log(1/a)$. Hence,

$$p\{d_\infty(\boldsymbol{\Omega}_{s,h}, \boldsymbol{\Omega}_{s,h}^d) > \epsilon\} \leq 1 - \exp\{\frac{-6ba^d}{\epsilon(1-a)}\} \leq \frac{6ba^d}{\epsilon(1-a)},$$

since $6ba^d/\{\epsilon(1-a)\} < 1$. □

Theorem 4. *Let*

$$f^L(\boldsymbol{y}_i) = \sum_{s=1}^{L}\sum_{h=1}^{2^s} \tilde{\pi}_{s,h}\mathcal{N}_D(\boldsymbol{y}_i; \boldsymbol{\mu}_{s,h}, \boldsymbol{\Phi}_{s,h}\boldsymbol{\Sigma}_{s,h}\boldsymbol{\Phi}_{s,h}^T + \sigma_s^2\boldsymbol{I})$$

denote the approximation at scale L, let $P(B) = \int_B f(\boldsymbol{y}_i)dy$ *and* $P^L(B) = \int_B f^L(\boldsymbol{y}_i)dy$*, for all* $B \subset \Re^D$ *denote the probability measures corresponding to density* $f(\boldsymbol{y}_i)$ *and* $f^L(\boldsymbol{y}_i)$*. Then we have,*

$$d_{TV}(P_L, P) < \left(\frac{a_S}{1+a_S}\right)^L,$$

where $d_{TV}(P_L, P)$ *denotes the total variation distance between* $P_L(B)$ *and* $P(B)$*.*

Proof. The total variation distance is given by

$$\begin{aligned}
d_{TV}(P_L, P) &= \sup_{B\in\Re^D} |P^L(B) - P(B)| \\
&= \sup_{B\in\Re^D} |\sum_{h=1}^{2^L} \tilde{\pi}_{s,h} N(B; \boldsymbol{\mu}_{s,h}, \boldsymbol{\Phi}_{s,h}\boldsymbol{\Sigma}_{s,h}\boldsymbol{\Phi}_{s,h}^T + \sigma_s^2\boldsymbol{I}) - ... \\
&\quad \sum_{s=L}^{\infty}\sum_{h=1}^{2^s} \pi_{s,h} N(B; \boldsymbol{\mu}_{s,h}, \boldsymbol{\Phi}_{s,h}\boldsymbol{\Sigma}_{s,h}\boldsymbol{\Phi}_{s,h}^T + \sigma_s^2\boldsymbol{I})| \\
&\leq \max\{\sum_{h=1}^{2^L} \tilde{\pi}_{s,h}, \sum_{s=L}^{\infty}\sum_{h=1}^{2^s} \pi_{s,h}\} \\
&= \max\left\{2^L(\frac{a_S}{1+a_S})^{L-1}\frac{1}{1+a_S}2^{-L}, \sum_{s=L}^{\infty} 2^s \frac{1}{1+a_S}(\frac{a_S}{2+2a_S})^s\right\} \\
&= \sum_{s=L}^{\infty}\frac{1}{1+a_S}(\frac{a_S}{1+a_S})^s \\
&= (\frac{a_S}{1+a_S})^L
\end{aligned}$$

□

B Posterior Conditional Derivation

Based on the likelihood function (A1), the derivation of conditional posterior of σ_s^{-2} is given by

$$\begin{aligned} p(\sigma_s^{-2}|-) &\propto (\sigma_s^{-2})^{a_\sigma-1}\exp(-b_\sigma\sigma_s^{-2})\prod_{y_i\in C_s}(\sigma_s^2)^{-D/2} \\ &\quad \exp\Big\{-\frac{1}{2}\sigma_s^{-2}(A_{s,h,i}-\sum_{j=1}^{d}(1-u_{s,h,j})(Z_{s,h,i}^{(j)})^2)\Big\} \\ &\propto (\sigma_s^{-2})^{Dn_s/2+a_\sigma-1} \\ &\quad \exp\Big\{-\sigma_s^{-2}[\frac{1}{2}\sum_{y_i\in C_s}(A_{s,h,i}-\sum_{j=1}^{d}(1-u_{s,h,j})(Z_{s,h,i}^{(j)})^2)+b_\sigma]\Big\}. \end{aligned}$$

The derivation of conditional posterior of $u_{s,h,m}$ is given by

$$\begin{aligned} p(u_{s,h,m}|-) &\propto \prod_{y_i\in C_{s,h}} u_{s,h,m}^{1/2}\exp\Big\{-\frac{1}{2}\sigma_s^{-2}u_{s,h,m}(Z_{s,h,i}^{(m)})^2\Big\} \\ &\quad u_{s,h,m}^{\prod_{j=1}^{m}\tau_{s,h,j}-1}\exp\{-u_{s,h,m}\}I_{(0,1)} \\ &\propto u_{m,s,h}^{\prod_{j=1}^{m}\tau_{s,h,j}+n_{s,h}/2-1} \\ &\quad \exp\Big\{-[1+\frac{1}{2}\sigma_s^{-2}\sum_{y_i\in C_{s,h}}(Z_{s,h,i}^{(m)})^2]u_{s,h,m}\Big\}I_{(0,1)}. \end{aligned}$$

The derivation of conditional posterior of $\tau_{s,h,m}$ is given by

$$\begin{aligned} p(\tau_{s,h,m}|-) &\propto (\prod_{j>m-1}u_{j,s,h})^{\tau_{s,h,j}}\exp\{-a_\tau\tau_{s,h,m}\}I_{[1,\infty)} \\ &\propto \exp\Big\{-[a_\tau-ln(\prod_{j>m-1}u_{s,h,j})]\tau_{s,h,m}\Big\} \end{aligned}$$

C Missing Data Imputation

Proposition 4. *For node (s,h), introduce augmented data $\boldsymbol{\eta}_i$ such that $(\boldsymbol{y}_i|\boldsymbol{\eta}_i,\boldsymbol{\Theta},s_i=s,h_i=h)\sim\mathcal{N}_D(\boldsymbol{\mu}_{s,h}+\boldsymbol{\Phi}_{s,h}\boldsymbol{\eta}_i,\sigma_s^2\boldsymbol{I}_D)$ and $(\boldsymbol{\eta}_i|\boldsymbol{\Theta},s_i=s,h_i=h)\sim\mathcal{N}_d(0,\boldsymbol{\Sigma}_{s,h})$, for $i=1,\ldots,n$. Then we have the conditional distribution with $\boldsymbol{\eta}_i$ marginalized out equal $(\boldsymbol{y}_i|\boldsymbol{\Theta},s_i=s,h_i=h)\sim\mathcal{N}_D(\boldsymbol{\mu}_{s,h}+\boldsymbol{\Phi}_{s,h}\boldsymbol{\Sigma}_{s,h}\boldsymbol{\Phi}_{s,h}^T,\sigma_s^2\boldsymbol{I}_D)$. Furthermore, conditional on $s_i=s$ and $h_i=h$ we have*

$$\boldsymbol{\eta}_i|\boldsymbol{y}_O,\boldsymbol{\Theta}\sim\mathcal{N}_d(\hat{\boldsymbol{\mu}}_\eta,\hat{\boldsymbol{\Sigma}}_\eta),\qquad \boldsymbol{y}_M|\boldsymbol{\eta}_i,\boldsymbol{y}_O,\boldsymbol{\Theta}\sim\mathcal{N}_{m_i}(\boldsymbol{\mu}_M+\boldsymbol{\Phi}_M\boldsymbol{\eta}_i,\sigma_s^2I_{m_i}),$$

where $\hat{\boldsymbol{\Sigma}}_\eta=\big(\boldsymbol{\Sigma}_{s,h}\boldsymbol{\Phi}_O^T\boldsymbol{\Phi}_O/\sigma_s^2+I\big)^{-1}\boldsymbol{\Sigma}_{s,h}$ and $\hat{\boldsymbol{\mu}}_\eta=\hat{\boldsymbol{\Sigma}}_\eta\boldsymbol{\Phi}_O^T(\boldsymbol{y}_O-\boldsymbol{\mu}_O)/\sigma_s^2$,

Proof. The proposition can be easily proved using Bayes rule. The joint density of $(\boldsymbol{y}_O,\boldsymbol{y}_M,\boldsymbol{\eta}_i|\boldsymbol{\Theta})$ is given by

$$\begin{aligned} p(\boldsymbol{y}_O,\boldsymbol{y}_M,\boldsymbol{\eta}_i|\boldsymbol{\Theta},s_i=s,h_i=h) &\propto \exp\Big\{-\frac{\|\boldsymbol{y}_i-\boldsymbol{\Phi}\boldsymbol{\eta}_i-\boldsymbol{\mu}\|_2}{2\sigma_s^2}-\frac{\boldsymbol{\eta}_i^T\boldsymbol{\Sigma}_{s,h}^{-1}\boldsymbol{\eta}_i}{2}\Big\} \\ &\propto \exp\Big\{-\frac{\|\boldsymbol{y}_M-\boldsymbol{\Phi}_M\boldsymbol{\eta}_i-\boldsymbol{\mu}_M\|_2}{2\sigma_s^2} \\ &\quad -\frac{\|\boldsymbol{y}_O-\boldsymbol{\Phi}_O\boldsymbol{\eta}_i-\boldsymbol{\mu}_O\|_2}{2\sigma_s^2}-\frac{\boldsymbol{\eta}_i^T\boldsymbol{\Sigma}_{s,h}^{-1}\boldsymbol{\eta}_i}{2}\Big\}. \end{aligned}$$

Hence the conditional density $(\boldsymbol{y}_M|\boldsymbol{\eta}_i,\boldsymbol{y}_O,\boldsymbol{\Theta},s_i=s,h_i=h)$ is given by

$$p(\boldsymbol{y}_M|\boldsymbol{\eta}_i,\boldsymbol{y}_O,\boldsymbol{\Theta},s_i=s,h_i=h)\propto\exp\Big\{-\frac{\|\boldsymbol{y}_M-\boldsymbol{\Phi}_M\boldsymbol{\eta}_i-\boldsymbol{\mu}_M\|_2}{2\sigma_s^2}\Big\}.$$

The marginal conditional density $(\boldsymbol{\eta}_i|\boldsymbol{y}_O, \boldsymbol{\Theta}, s_i = s, h_i = h)$ is given by

$$\begin{aligned}\mathrm{p}(\boldsymbol{\eta}_i|\boldsymbol{y}_i^O, \boldsymbol{\Theta}, s_i = s, h_i = h) &\propto \int \mathrm{p}(\boldsymbol{y}_M, \boldsymbol{\eta}_i|\boldsymbol{y}_O)\mathrm{d}\boldsymbol{y}_M \\ &\propto \exp\left\{\frac{\|\boldsymbol{y}_O - \boldsymbol{\Phi}_O\boldsymbol{\eta}_i - \boldsymbol{\mu}_O\|_2}{2\sigma_s^2} - \frac{\boldsymbol{\eta}_i^T\boldsymbol{\Sigma}_{s,h}^{-1}\boldsymbol{\eta}_i}{2}\right\}.\end{aligned}$$

□

To finish the missing data imputation algorithm, the conditional posterior distribution of the membership variable (s_i, h_i) of partially observed subject i, $p(s_i, h_i|\boldsymbol{y}_O, \boldsymbol{\Theta})$ is needed. $\boldsymbol{y}_M$ has been marginalized out to reduce the sample autocorrelation, and the distribution is given by

$$\begin{aligned}\mathrm{p}(s_i, h_i|\boldsymbol{y}_O, \boldsymbol{\Theta}) &\propto \int p(\boldsymbol{y}_M, \boldsymbol{y}_O, \boldsymbol{\Theta}, s_i, h_i)\mathrm{d}\boldsymbol{y}_M \\ &\propto \int \pi_{s_i,h_i}\mathcal{N}_D(\boldsymbol{y}_i; \boldsymbol{\mu}_{s_i,h_i}, \boldsymbol{\Phi}_{s_i,h_i}\boldsymbol{\Sigma}_{s_i,h_i}\boldsymbol{\Phi}_{s_i,h_i}^T + \sigma_{s_i}^2\mathbf{I})\mathrm{d}\boldsymbol{y}_M.\end{aligned}$$

With a slight abuse of notation, we write $\boldsymbol{\Phi}$ as $\boldsymbol{\Phi}_{s_i,h_i}$, $\boldsymbol{\Sigma}$ as $\boldsymbol{\Sigma}_{s_i,h_i}$, σ^2 denote $\sigma_{s_i}^2$ and $\boldsymbol{\mu}$ as $\boldsymbol{\mu}_{s_i,h_i}$. By properties of multicariate Gaussian, we have

$$\int \mathcal{N}_D(\boldsymbol{y}_i; \boldsymbol{\mu}, \boldsymbol{\Phi}\boldsymbol{\Sigma}\boldsymbol{\Phi}^T + \sigma^2\mathrm{I})\mathrm{d}\boldsymbol{y}_M = \mathcal{N}_{D-m_i}(\boldsymbol{y}_O; \boldsymbol{\mu}_O, \boldsymbol{\Phi}_O\boldsymbol{\Sigma}\boldsymbol{\Phi}_O^T + \sigma^2\boldsymbol{I}).$$

Hence we have $p(s_i, h_i|\boldsymbol{y}_O, \boldsymbol{\Theta}) \propto \mathcal{N}_{D-m_i}(\boldsymbol{y}_O; \boldsymbol{\mu}_O, \boldsymbol{\Phi}_O\boldsymbol{\Sigma}\boldsymbol{\Phi}_O^T + \sigma^2\boldsymbol{I})$. Directly computing this value includes inverting a $(D - m_i) \times (D - m_i)$ matrix, which is computational intractable when $D - m_i$ is large. With basic linear algebra, we have

$$\begin{aligned}\left|\boldsymbol{\Phi}_O\boldsymbol{\Sigma}\boldsymbol{\Phi}_O^T + \sigma^2\boldsymbol{I}\right| &= (\sigma^2)^{D-m_i}\left|\boldsymbol{I} + \boldsymbol{\Sigma}\boldsymbol{\Phi}_O^T\boldsymbol{\Phi}_O/\sigma^2\right|, \\ \left(\boldsymbol{\Phi}_O\boldsymbol{\Sigma}\boldsymbol{\Phi}_O^T + \sigma^2\boldsymbol{I}\right)^{-1} &= \frac{\boldsymbol{I}}{\sigma^2} - \frac{\boldsymbol{\Phi}_O\left(\boldsymbol{I} + \boldsymbol{\Sigma}\boldsymbol{\Phi}^T\boldsymbol{\Phi}_O/\sigma^2\right)^{-1}\boldsymbol{\Sigma}\boldsymbol{\Phi}_O^T}{\sigma^4}.\end{aligned}$$

Hence we have

$$\begin{aligned}&\mathcal{N}_{D-m_i}(\boldsymbol{y}_O; \boldsymbol{\mu}_O, \boldsymbol{\Phi}_O\boldsymbol{\Sigma}\boldsymbol{\Phi}_O^T + \sigma^2\boldsymbol{I}) \\ =&(2\pi\sigma^2)^{-(D-m_i)/2}\left|\boldsymbol{I} + \boldsymbol{\Sigma}\boldsymbol{A}/\sigma^2\right|^{-1/2} \\ &\times \exp\left\{-\frac{B_i}{2\sigma^2} + \frac{\boldsymbol{C}_i^T\left(\boldsymbol{\Sigma}^{-1} + \boldsymbol{A}/\sigma^2\right)^{-1}\boldsymbol{C}_i}{2\sigma^4}\right\}\end{aligned} \tag{A2}$$

where $\boldsymbol{A} = \boldsymbol{\Phi}_O^T\boldsymbol{\Phi}_O$, $B_i = \|\boldsymbol{y}_O - \boldsymbol{\mu}_O\|_2$ and $\boldsymbol{C}_i = \boldsymbol{\Phi}_O^T(\boldsymbol{y}_O - \boldsymbol{\mu}_O)$. Note that $\boldsymbol{A}$, B_i and $\boldsymbol{C}_i$ can be computed before the MCMC algorithm with a computational cost being $O\big((D - m_i)d\big)$. Within the MCMC, the cost to compute (A2) is only $O(d^3)$.

D Simulation Studies

In the missing data imputation simulatoin study, we simulated 100 independent samples of size $n = 600$ from different scenarios as follows.

Scenario 1-6: Data $\boldsymbol{y}_i$, for $i = 1, \ldots, 600$, were generated from $\mathcal{N}_D(0, \boldsymbol{\Lambda}\boldsymbol{\Lambda}^T + \sigma^2\boldsymbol{I})$. $\boldsymbol{\Lambda}$ is a $D \times p$ matrix with each entry generated from $\mathcal{N}(0, 25)$ and $10\sigma^2$ was generated from $\chi_{(1)}$. This scenario includes different cases where $p \in \{10, 50\}$, $D \in \{5000, 10000, 15000\}$ and with or without a 20% missing data. We fixed the upper bound to $d = 100$.

Scenario 7-9: 3–D data $\boldsymbol{\eta}_i$, for $i = 1, \ldots, 600$, were generated on the Swissroll with Gaussian noise distributed as $\mathcal{N}(0, 2.5 \times 10^{-5})$ along each dimension. Data $\boldsymbol{y}_i$, for $i = 1, \ldots, 600$, were obtained by $\boldsymbol{y}_i = \boldsymbol{\Lambda}\boldsymbol{\eta}_i$ where $\boldsymbol{\Lambda}$ were generated in the same way as in Scenario 1. This scenario includes different cases where $D \in \{5000, 10000, 15000\}$ and with or without a 20% missing data. We fixed the upper bound to $d = 10$.

The average inclusion probabilities of each presetted dimensions were computed in the following way. Let $\mathcal{R}^t_{s,h}$ denotes the set of retained column indices of node (s,h) at the tth iteration, and let (s^t_i, h^t_i) denote the node index of the ith observation at the tth iteration. Then the inclusion probability of dimension $j = 1, 2, \ldots, 10$ in scenario 2 is given by

$$p_j^{inclu} = \frac{1}{n_{adapt} \times N} \sum_{t:\ adapt} \sum_{i=1}^{N} I_{(j \in \mathcal{R}^t_{s^t_i, h^t_i})}$$

where n_{adapt} denotes the number of adaptation steps during the MCMC collection interval.